www.czasopisma.pan.pl PAN POLSKA AKADEMIA NAUK www.journals.pan.pl

Arch. Min. Sci. **63** (2018), 1, 149-163

Electronic version (in color) of this paper is available: http://mining.archives.pl

DOI 10.24425/118892

BOGUSŁAW PTASZYŃSKI*#, RAFAŁ ŁUCZAK*,
PIOTR ŻYCZKOWSKI*, ZBIGNIEW KUCZERA*

THERMODYNAMIC PROCESSES OF THE AIR FLOWING THROUGH A VENTILATION SHAFT IN UNDERGROUND MINES

PROCESY TERMODYNAMICZNE POWIETRZA W SZYBIE WENTYLACYJNYM KOPALNI

The paper describes the application of the Mollier diagram and the procedure of its modification, presented in the article (Ptaszyński, 2016), for the analysis of thermodynamic transitions of the humid air stream flowing through mine ducts in conditions of highly variable static pressure. Exemplary measurement data have been used to perform the scrutiny of thermodynamic processes of the air during its flow as well as to determine the type of mass water sources occurring there as result of water vapour condensation, and their mass flow rates.

Keywords: Mollier diagram, thermodynamic transitions of the air, condensation of water vapour, mass water source

W artykule wykorzystano wykres Molliera i zaproponowaną w pracy (Ptaszyński, 2016) procedurę jego modyfikacji do analizy przemian termodynamicznych strumienia powietrza wilgotnego płynącego w przewodach o istotnie zmieniającym się ciśnieniu statycznym. Wykorzystując przykładowe dane pomiarowe wykonano analizy procesów termodynamicznych powietrza zachodzących na drodze jego przepływu, określono charakter występujących na niej masowych źródeł wody pochodzącej z kondensacji pary wodnej i ich wydajności masowe.

Słowa kluczowe: wykres Molliera, przemiany termodynamiczne powietrza, kondensacja pary wodnej, źródło masowe wody

1. Introduction

The air from the underground mines is discharged to the surface through vertical ducts called exhausting shafts. The airflow is usually forced by main ventilation system fans installed on the

* AGH UNIVERSITY OF SCIENCE AND TECHNOLOGY, FACULTY OF MINING AND GEOENGINEERING, AL. A. MICKIEWICZA 30, 30-059 KRAKÓW, POLAND

Corresponding author: ptaszyns@agh.edu.pl

surface in the vicinity of ventilation shafts. The fans work as intake systems generating in the exhausting shaft negative pressure of significant value when compared to the one on the surface and at the bottom of the shafts. Parameters of the latter may vary: cross sections of almost all of them is round, their diameters range from 6,0 to 9,0 m and their lengths do not exceed 1300 metres. However, the growing need to extract natural resources situated deeper underground, results in increasingly longer shafts. Humid air discharged through them to the surface is characterised by very high relative humidity ranging from 95 to 100% and temperature whose values, depending on the level at which the air flows into the shaft, usually ranges from 20°C to 32°C. Thermodynamic parameters of the air entering a ventilation shaft at a given level most often do not change over a longer period of time, however, volumetric flow rates of such streams may vary. A ventilation shaft structure usually includes several levels situated at different depths, and its surface outlet opening, called the outset, which has the airflow choked with flaps. A ventilation duct connected with the ventilation shaft through a ventilation pipe is responsible for discharging used air from underground excavations to the surface. During its flow along the shaft, humid air undergoes two thermodynamic transitions: cooling of the whole air stream and mixing of the flowing humid air stream with the one entering the shaft at a given level. These phenomena consequently lead to condensation of the water vapour contained in humid air streams, which may contribute to the occurrence of a mass water source in vertical and inclined ducting such as a ventilation shaft, a ventilation pipe or a ventilation duct. Mass water sources come in two types (Ptaszyński, 2016):

- a mass water source continuous along the flow of the air, appearing in the sections where condensation phenomenon accompanying cooling process takes place,
- a mass water source localised on the airflow path, occurring in those places of mixing air streams where there are favourable conditions for induced condensation phenomenon. The process of mixing air streams takes place at air intakes situated at a given level in the shaft or at the intersection of the shaft with a ventilation pipe where the air flowing from the mine along the shaft mingles with the one originating from the so-called "external air losses", and is limited to a section whose length is equal to the height of the ducting connected to the shaft. Potential vapour condensation accompanying the mixing process is also a distributed water source. However, due to a relatively short length of this section (in comparison with other shaft section where vapour condensation phenomenon occurs) and difficulty to determine the water source output form as a function of distance, for the purpose of the following paper it is assumed that they are all localised water sources occurring in places where air stream mixing can be observed.

The occurrence of water drops from water vapour condensation in humid air flowing along ducting in the upwards direction, renders determining the definition of such mixture difficult. If water drops velocity does not equal zero, then the flow of air and water can be described as two-phase one (Ptaszyński, 2016). However, if the velocity of every water drop is equal to zero, then, the humid airflow is single-phase one due to the "filling" of immovable water droplets suspended in the return airway. Such flow phenomenon is known as gas fluidization (Orzechowski et al., 2009).

The relevant question is whether inflow water sources induced by condensation phenomenon can be found in the return path of humid air: in a shaft and ventilation duct with highly variable static pressure; what are the types of the sources and their mass output. The answer enables pinpointing those sections of the return airway where the gas flow is of one-phase character and those sections where the airflow is two-phase or single-phase with "filling" called in the mining jargon, "a loop water seal".

However, specifying that relevant information is not an easy task as mining measurement procedures of ventilation and thermodynamic air parameters are performed with the use of instruments intended for determining one-phase gas stream parameters (Wacławik, 2010). Thus, even with the obtained measurement results of the air parameters in a ventilation shaft, it is difficult to determine without ambiguity if the above mentioned processes occur in the shaft and in which shaft section exactly.

The paper utilizes the modification of the Mollier diagram for airflows with highly variable static pressure described in the article (Ptaszyński, 2016), to analyse the thermodynamic processes of discharged humid air on its return airways as well as its parameters.

Using ventilation and thermodynamic measurement data of the air carried away to the surface through the underground mine ventilation shaft, the paper presents computational procedures which have allowed to determine the locations as well as the type (distributed, localised) of the occurrence of underground water sources induced by water vapour condensation in the air.

2. Measurement data of air streams carried away to the surface through a ventilation shaft and a ventilation duct

Figure 1 shows a diagram depicting the system of air discharge from a mine which consists of a two-level ventilation shaft, a ventilation pipe and a ventilation duct.

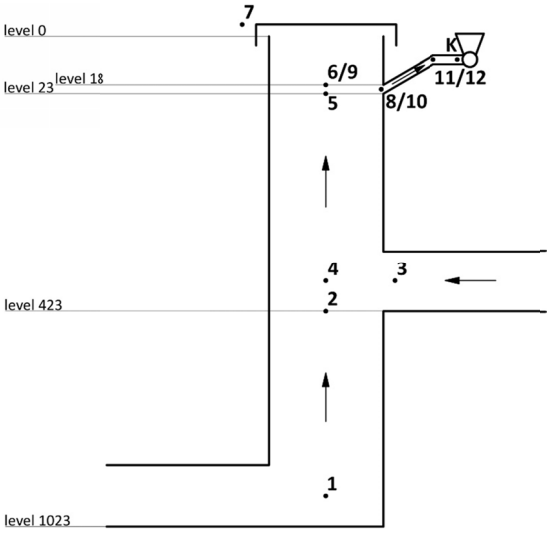

Fig. 1. Air discharge pathway with marked points assigned to a suitable cross section of the air stream flowing inside it

The analysed ventilation shaft with the diameter of 7 m and a cross section area of $F = 38,48$ m^2, is located at the depth of 1030 m. The floor of the lower shaft level transporting the in-

coming air is located at 1023 m, the floor of the higher level – at 423 m, while the floor of the ventilation pipe – at 23 m. The linear pressure loss coefficient is $\lambda = 0{,}02$ (for turbulent developed flow). The height of the both shaft bottoms is 6m, and the diameter of the ventilation pipe is 5 m. The pipe's length is equal to $l_{pipe} = 28$ m and its slope to $\alpha = 45°$. The 45-metre-long ventilation duct has a rectangular cross section of dimensions 4×5 m and the slope equal to $\beta = 5°$. The results of the performed measurements and calculations of the ventilation and thermodynamic parameters are the following:

- the incoming airflow at 1023 level:
  - barometric pressure $p_1 = 110000$ Pa,
  - dry-bulb temperature $t_{s1} = 29°C$,
  - wet-bulb temperature $t_{w1} = 28{,}5°C$,
  - specific humidity of air $x_1 = 0{,}02258$ kg/kg,
  - air density $\rho_1 = 1{,}2517$ kg/m^3,
  - volumetric stream of humid air fed into the shaft $\dot{V}_1 = 166{,}67$ m^3/s,
  - mass stream of humid air $\dot{m}_1 = 208{,}62$ kg/s,
  - mass stream of dry air $\dot{m}_{s1} = 204{,}01$ kg/s.
- the incoming airflow at the 423 level:
  - barometric pressure $p_3 = 98500$ Pa,
  - dry-bulb temperature $t_{s3} = 26°C$,
  - wet-bulb temperature $t_{w3} = 25°C$,
  - specific humidity of air $x_3 = 0{,}02024$ kg/kg,
  - air density $\rho_3 = 1{,}1336$ kg/m^3,
  - volumetric stream of humid air fed into the shaft $\dot{V}_3 = 166{,}67$ m^3/s,
  - mass stream of humid air $\dot{m}_3 = 188{,}93$ kg/s,
  - mass stream of dry air $\dot{m}_{s3} = 185{,}18$ kg/s.
- external air is sucked from the surface into the shaft through a sealed-off outset.

Barometric pressure at the surface is $p_7 = 98600$ Pa. The conducted research took into account air parameters characteristic for winter and summer periods, which are as follows:

- in winter:
  - dry-bulb temperature $t_{s7} = -20°C$,
  - wet bulb-temperature $t_{w7} = -20°C$,
  - specific humidity of air $x_7 = 0{,}0079$ kg/kg,
  - air density $\rho_7 = 1{,}35645$ kg/m^3,
  - mass flow rate of external air intake accounts for 10% of the mass flow rate of air discharged through the shaft (section 4-5), i.e. $\dot{m}_7 = 0{,}1(\dot{m}_1 + \dot{m}_3)$.
- in summer:
  - dry-bulb temperature $t_{s7} = 24°C$,
  - wet-bulb temperature $t_{w7} = 21°C$,
  - specific humidity of air $x_7 = 0{,}01484$ kg/kg,
  - air density $\rho_7 = 1{,}14597$ kg/m^3,
  - mass flow rate of external air intake accounts for 10% of the mass flow rate of air discharged through the shaft (section 4-5), i.e. $\dot{m}_7 = 0{,}1(\dot{m}_1 + \dot{m}_3)$.

Apart from the above mentioned measurements, additional studies have been conducted at the end of sections (1-2 and 4-5), at the cross section of the shaft below the air inlet at a higher

level (cross section 2) as well as below the ventilation pipe inlet (cross section 5). The results of the measurements are as follows:

- barometric pressure $p_2 = p_3 = p_4 = 98500$ Pa,
- dry and wet-bulb temperature $t_{s2} = t_{w2} = 24°C$,
- air density $\rho_2 = 1{,}14332$ kg/m^3,
- volumetric stream of humid air $\dot{V}_2 = \frac{\dot{m}_2}{\rho_2} = 182{,}469\,\mathrm{m}^3/\mathrm{s}$,
- barometric pressure $p_5 = p_6 = p_K = 93600$ Pa,
- dry and wet bulb temperature $t_{s5} = t_{w5} = 22°C$,
- air density $\rho_5 = 1{,}0941$ kg/m^3,
- volumetric stream of humid air $\dot{V}_5 = \frac{\dot{m}_2 + \dot{m}_3}{\rho_5} = 363{,}358\,\mathrm{m}^3/\mathrm{s}$.

If the airflow at the cross sections 2 and 5 was single-phase one (saturated humid air), then the average air velocity in those cross sections would be equal to $v_2 = \frac{\dot{V}_2}{F} = 4{,}74\,\mathrm{m/s}$ and $v_5 = \frac{\dot{V}_5}{F} = 9{,}44\,\mathrm{m/s}$.

As it has been concluded above, the measurements recorded at the cross sections of the shafts 2 and 5 do not determine unambiguously whether there is a single-phase saturated humid airflow or two-phase one, where in addition to the vapour saturated air stream constituting the carrier gas phase, there is a stream of fluid, produced in the process of vapour condensation in the air pathway. Ventilation measuring instruments commonly used in mining nowadays are not capable of determining the presence of water drops in the air. Therefore the authors of the paper propose using the thermodynamic method which allows to detect the presence of the water vapour condensation in sections (1-2) and (4-5) of the ventilation shaft and precisely pinpoint the length at which the phenomenon occurs. The method involving the Mollier diagram presented in the paper (Ptaszyński, 2016) should be performed in the order of the airflow as it is discharged from the mine.

3. Thermodynamic transitions of air occurring during its flow through a ventilation shaft

The Mollier diagram is constructed for precisely defined static pressure (Pudlik, 2011; Wacławik, 2010), with the value of 0, 1 MPa (1bar) most commonly used. However, appropriate software (IX-CHART) makes it possible to generate a diagram for a different analysed value of the static pressure but not such that would involve 'fluent' adjustments of the pressure values changing due to thermodynamic transitions. During the discharge of the air (Fig. 1) as a result of the altering height, significant variations of its pressure can be observed. In such cases, the Mollier diagram cannot be directly applied to analyse thermodynamic transitions of the air.

As it has already been proven in the paper (Ptaszyński, 2016), the change of pressure does not affect the position of the point on the Mollier diagram, which represents a thermodynamic state of a medium which can be single-phase – as in the case of humid air or two-phase one – haze air containing water mist or ice fog. However, it induces a change in the output diagram of the region constituted by points describing thermodynamic states of humid air as well as the

zone assigned to the haze medium (two-phase one). As a result, the placement of the relative humidity curve equal 1 separating those two regions with the new pressure values, is different. An additional consequence of the pressure variation is the change of the constant relative humidity as well as the water vapour pressure curves.

Humid air transitions can be presented graphically by means of the Mollier diagram, however, constant pressure can be observed only during mixing transitions. Heating and cooling transitions of the humid air flowing through the underground mine excavations, may occur in a wide range of conditions, from the ones satisfying the so-called requirements of constant pressure to cases where pressure values change substantially. Thermodynamic transitions of the air flowing through the shaft take place in the latter circumstances.

The placement of izentalp (i = const) and izohigr (x = const) grids on the Mollier diagram is not affected by pressure fluctuations. However, isothermal characteristics for the thermodynamic states of the single-phase humid air region are different from the ones covering the thermodynamic states of the two-phase region (containing water mist and ice fog).

The variability of the pressure causes different placement not only of the saturation curve $\varphi = 1$ but also of relative humidity curves. Consequently, a point which on the Mollier diagram is situated in the single-phase region may be covered by the two-phase region and vice versa. Fig. 2 illustrates the method of creating new relative humidity curves of the water vapour saturated air for two different values of static air pressure.

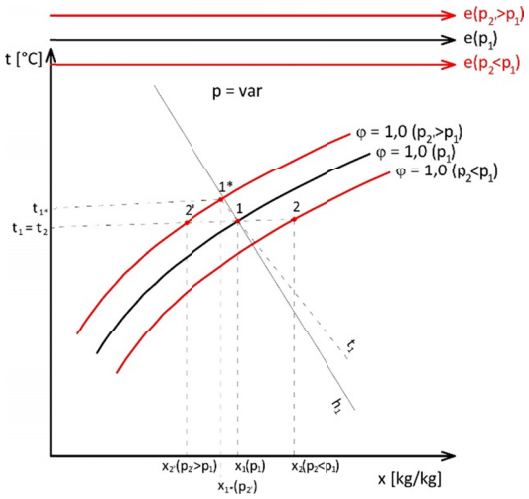

Fig. 2. Influence of air static pressure changing on thermodynamic state of air (Ptaszyński, 2016)

Cooling and mixing transitions observed on the return airway have been presented in Fig. 3, with constant and variable static pressure.

The increased pressure results in reducing the existing area which includes the points constituting possible thermodynamic states of humid air with fixed pressure p_1. As can be seen in Fig. 2, the relative humidity curve equal 1 for the new increased pressure is situated to the left of the relative humidity curve equal 1 for pressure p_1. Consequently, point 1 depicting a thermodynamic state of a given medium on the Mollier diagram, remaining in the same position,

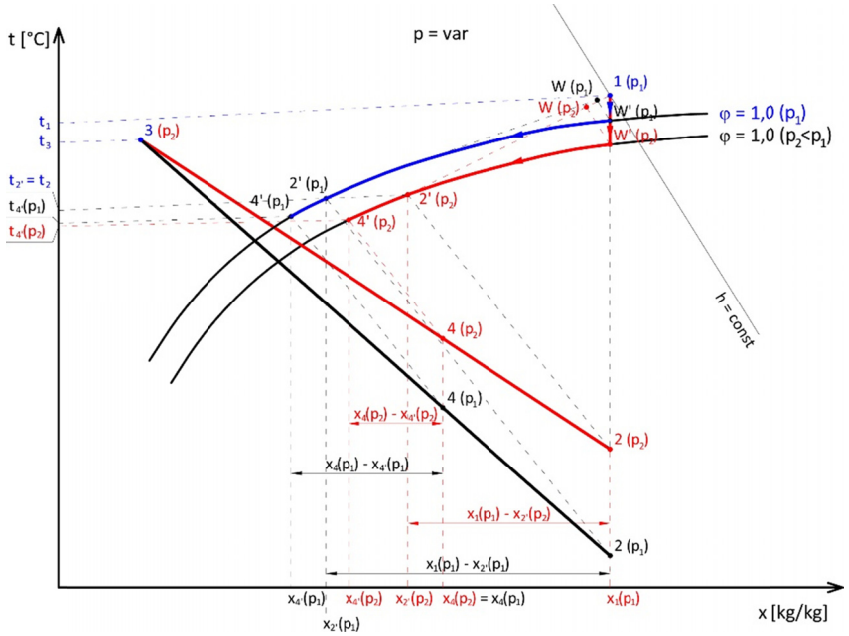

Fig. 3. Thermodynamic transformations, which are going in the upcast ventilation with unchanged and changed pressure of air (Ptaszyński, 2016)

will be included in the water mist region. The point specifying a thermodynamic state of one of the mist components, i.e. water vapour saturated air, has been denoted in Fig. 1 as pt. 1*, and its coordinates t^*_1, x^*_1 can be calculated from the following formulas (1) and (2):

$$t^*_1 \cdot \left[\frac{0,622 \cdot 610,6 \cdot \exp\left(\frac{17,27 t^*_1}{237,3 + t^*_1} \right) \cdot \left(c_{pp} - c_{pw} \right)}{a \cdot p_1 - 610,6 \cdot \exp\left(\frac{17,27 t^*_1}{237,3 + t^*_1} \right)} + x_1 \cdot c_{pw} + c_p \right] =$$
$$= t_1 \left(c_p + x_1 \cdot c_{pp} \right) + x_1 \left(2502,5 - 2,386 \cdot t^*_1 \right) +$$
$$- \frac{0,622 \cdot 610,6 \cdot \exp\left(\frac{17,27 t^*_1}{237,3 + t^*_1} \right) \cdot \left(2502,5 - 2,386 \cdot t^*_1 \right)}{a \cdot p_1 - 610,6 \cdot \exp\left(\frac{17,27 t^*_1}{237,3 + t^*_1} \right)} \tag{1}$$

$$x^*_1 = \frac{0,622 \cdot 610,6 \cdot \exp\left(\frac{17,27 t^*_1}{237,3 + t^*_1} \right)}{a \cdot p_1 - 610,6 \cdot \exp\left(\frac{17,27 t^*_1}{237,3 + t^*_1} \right)} \tag{2}$$

The equation (1) is transcendental, thus, calculating the temperature t_1^*, which is one of the coordinates of pt. 1^* requires numerical calculations. The value of the temperature is higher than t_1, if $a > 1$, which occurs when the pressure increases from p_1 to p_2 $\left(a = \frac{p_2}{p_1} \right)$.

Having calculated the temperature t_1^* of the vapour saturated air at the increased pressure, it is possible to obtain the value of its specific humidity x_1^* with the formula (2). This facilitates the calculation of the value $(x_1 - x_1^*)$ and the mass stream of the condensing water vapour in the stream of flowing air with increased static pressure parameters is calculated therefrom.

In the analysed numerical example air stream cooling processes can be observed in sections 1-2, 4-5 and 8-11 (10-12), while the mixing processes occur automatically at the shaft air inlets at the levels of 423 m and 23 m.

The analysis of thermodynamic transitions of air taking place in the presented shaft, has been conducted in accordance with the described procedure taking into account air pressure variability. Figure 4 illustrates the cooling process of the air flowing through section 1-2 and mixing of the air streams of the parameters shown at pt. 2 and pt. 4, resulting in creating a mixture of the parameters described at pt. 4.

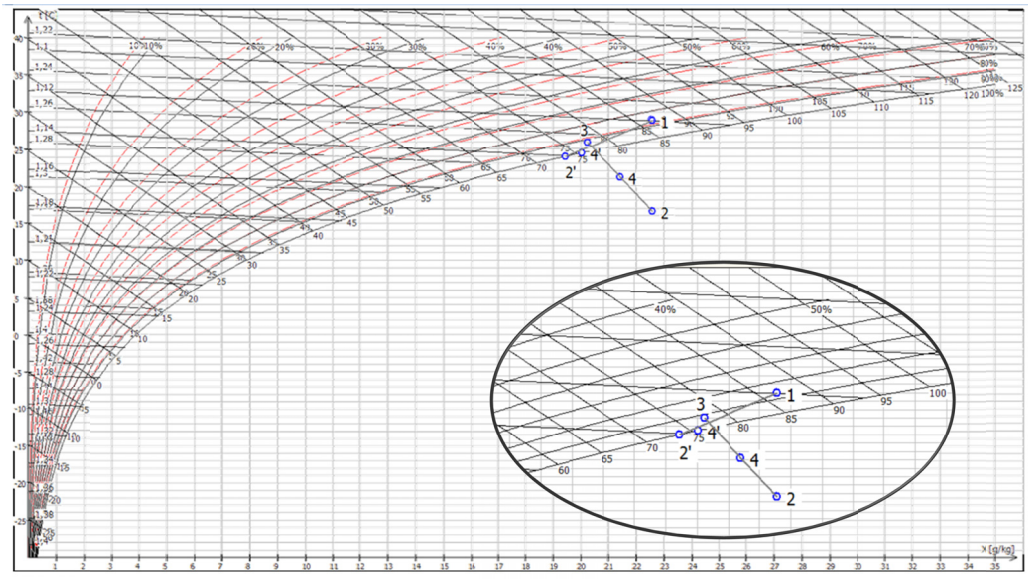

Fig. 4. Cooling and mixing transitions of the air streams in section 1-4 of the exhausting shaft

Due to the scale and in order to assure the legibility of the diagram, the image of the analysed area has been magnified and placed in the lower right corner.

Figure 5 depicts cooling transitions of air in sections 4-5, 8-11 (10-12) during summer and winter periods.

Table 1 summarises thermodynamic parameters of the air recorded at the specific points shown in Fig. 1.

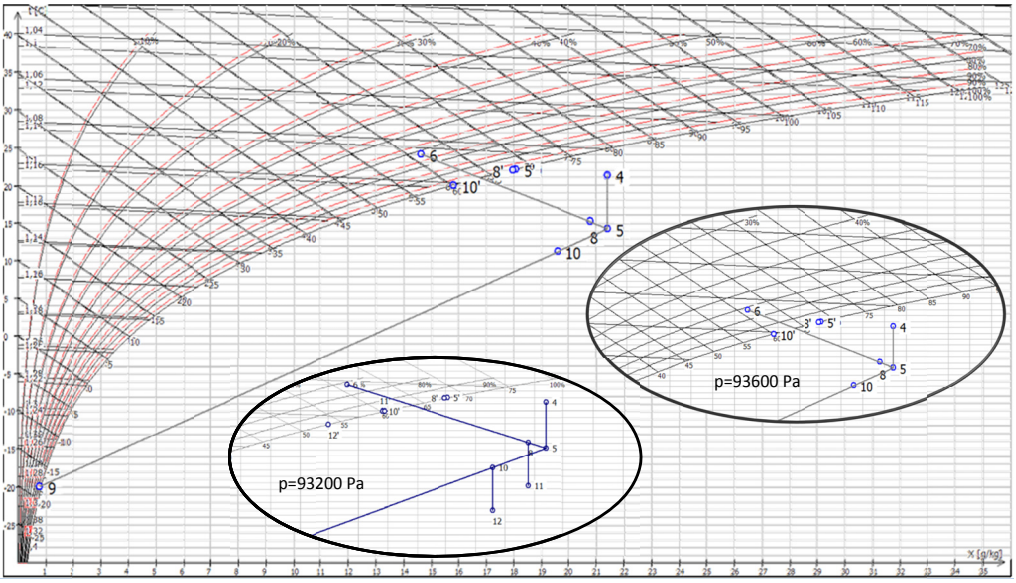

Fig. 5. Cooling and mixing transitions of air streams in sections 4-11 (4-12) of the exhausting shaft

TABLE 1

Parameters of the air flowing through the exhausting shaft

Point	t_s, °C	t_w, °C	x, kg/kg	φ, %	h, kJ/kg	p, Pa
1	29,0	28,5	0,02258	96,25	86,8	110000
2	24,0	24,0	0,02258	100,00	73,9	98500
2’	24,0	24,0	0,01942	100,00	73,6	98500
3	26,0	25,0	0,02024	92,30	77,8	98500
4	24,5	24,5	0,02140	100,00	75,8	98500
4’	24,5	24,5	0,02000	100,00	75,7	98500
5	22,0	22,0	0,02140	100,00	68,4	93600
5’	22,0	22,0	0,01810	100,00	68,1	93600
6	24,0	20,4	0,01486	73,20	62,0	93600
9	–20,0	–20,1	0,00079	94,50	–18,2	93600
7 SUMMER	24,0	21,0	0,01486	77,13	61,9	98600
7 WINTER	–20,0	–20,0	0,00079	100,00	–18,2	98600
8	21,9	21,9	0,02080	100,00	67,8	93600
8’	21,9	21,9	0,01790	100,00	67,7	93600
10	19,9	19,9	0,01950	100,00	60,4	93600
10’	19,9	19,9	0,01580	100,00	60,0	93600
11	19,9	19,9	0,02080	100,00	60,8	93200
11’	19,9	19,9	0,01590	100,00	60,4	93200
12	17,9	17,9	0,01950	100,00	53,9	93200
12’	17,9	17,9	0,01400	100,00	53,5	93200

4. Location and type of water sources induced by the phenomenon of water vapour condensation

The performed calculations demonstrate that during the air cooling process in section 1-2, water vapour condensation occurs at a distance of approximately 80 m from pt. 1. The distance can be calculated from the following dependence:

$$L_{1-W} = d_{1-W} L_{1-2},\ \text{m} \tag{3}$$

where:

d_{1-W} — is the ratio of the length of $1-W$ segment to the length of the segment connecting pt. 1 and pt. 2' on the Mollier diagram (Fig. 3). The point W, as it has been shown in Fig. 3, is the orthogonal projection of the point W^* onto the segment 1-2'. For the numerical example it is designated as $d_{1-W} = 0{,}133(3)$.

L_{1-2} — is the length of section 1-2 of the shaft, which in the presented example is equal to 600 m

Water vapour condensation region with the length of 520 m occurs in the 600-metre-long section $(1-2)$ corresponding to the section $(W-2)$ illustrated in Fig. 3. The phenomenon of water vapour condensation from flowing air can be represented as a continuous function. Unit mass output of the water source in this section of the shaft can be expressed as:

$$\dot{m}_{W_j(W-2)} = \dot{m}_{s(1-2)} \frac{x_1 - x_{2'}}{s_2 - s_W},\ \text{kg/(s}\cdot\text{m)} \tag{4}$$

where:

$\dot{m}_{s(1-2)}$ — mass stream of dry air in the shaft section 1-2, kg/s, which can be calculated from the dependence (5):

$$\dot{m}_{s(1-2)} = \frac{\dot{m}_{(1-2)}}{1 + x_1},\ \text{kg/s} \tag{5}$$

$\dot{m}_{(1-2)}$ — mass stream of humid air in the shaft section 1-2, kg/s,

x_1 — specific humidity of air stream at the beginning of the shaft section 1-2, kg/kg, the value calculated on the basis of the measurement data from the dependence:

$$x_1 = 0{,}622 \frac{e_1}{p_1 - e_1},\ \text{kg/kg} \tag{6}$$

e_1 — water vapour pressure in humid air at pt. 1, Pa,

$x_{2'}$ — specific humidity of vapour saturated air stream at the end of the shaft section 1-2, kg/kg, the value read from the Mollier diagram,

s_2 — distance coordinate corresponding to the position of pt. 2 in the shaft, m,

s_W — distance coordinate corresponding to the position of the initial point of water vapour condensation, m.

Using the dependencies (4, 5, 6) a unit mass flux of the distributed water source occurring in W-2 section of the shaft, has been calculated:

$$\dot{m}_{W_j(W-2)} = \dot{m}_{s(1-2)} \frac{x_1 - x_{2'}}{s_2 - s_W} = 204{,}01 \left[\frac{0{,}02258 - 0{,}01942}{600 - 80} \right] = 0{,}001240\ \text{kg/(s}\cdot\text{m)}$$

The phenomenon of mixing two air streams: the one flowing through the shaft with the parameters defined at pt. 2 with the humid one, whose parameters are specified at pt. 3 (Fig. 1), occurs at the intersection of the shaft with the shaft bottom situated at the depth of 432 m.

The stream characterised at pt. 2 is a two-phase flow (water mist) with the pressure equal to that of the incoming humid air at this level. The process of mixing such air streams depicted on the Mollier diagram for given pressure, makes it possible to determine thermodynamic parameters of the resultant stream specified at pt. 4 (Fig. 4). The placement of points 4 and 4' indicates that the resultant airflow is two-phase in character and contains humid air as well as water droplets. However, it is not conclusive if the air stream mixing process itself induces the occurrence of the localised mass water source situated at the cross section of s_2 coordinate. The mass output of this water source can be calculated from the dependence:

$$\dot{m}_{W(2-3)} = \left(\dot{m}_{s1} + \dot{m}_{s3}\right)\left(x_4 - x_{4'}\right) - \dot{m}_{s1}\left(x_2 - x_{2'}\right), \text{ kg/s} \tag{7}$$

where:

x_4, x_2 — moisture content in mixing air streams read from the Mollier diagram corresponding to the pressure in the mixing region at pt. 4 and pt. 2, kg/kg

$x_{4'}$, $x_{2'}$ — specific humidity of water vapour saturated air streams read from the Mollier diagram corresponding to the pressure in the mixing region, at pt. 4' and pt. 2', kg/kg

$\dot{m}_{s3}$ — mass stream of dry air fed at pt. 3 into the shaft, kg/s.

The necessary condition for the occurrence of a mass water source resulting from two water streams mixing, is satisfying the inequality:

$$\frac{x_2 - x_{2'}}{x_4 - x_{4'}} < \frac{\dot{m}_{s1} + \dot{m}_{s3}}{\dot{m}_{s1}} \tag{8}$$

The value of the left side of the inequality (8) is greater than the right one which has been calculated on the basis of the output data from the presented example, which is validated by the statement that the process of mixing of air streams at an upper shaft bottom determines the presence of the local mass water relief at pt. 2 (in cross section 2 in the shaft), whose value can be estimated from the dependence (7), where:

$$\dot{m}_{W(2-3)} = (204{,}01 + 185{,}18)(0{,}0214 - 0{,}0200) + \\ - 204{,}01(0{,}02258 - 0{,}01942) = -0{,}09977 \text{ kg/s}$$

Mixing of the haze air stream containing water mist with humid air fed into the shaft at a higher level, causes local occurrence of a water relief, the so-called a negative mass water source with the output $\dot{m}_{W(2-3)} = -0{,}09977$ kg/s.

The flow of the water mist can still be observed in section 4-5 of the shaft, as pt. 4 illustrating the thermodynamic state of this medium lies in the two-phase region of the Mollier diagram. The air is again cooled and its pressure decreases significantly on the 400-metre-long section 4-5 as shown in Fig. 5. Vapour condensation process takes place in section 4-5, which determines the presence of the mass water source in the given airflow pathway. The mass water source can be presented as a continuous function of the distance. A unit mass flux of this water source is:

$$\dot{m}_{W_j(4-5)} = \dot{m}_{s(4-5)} \frac{x_{4'} - x_{5'}}{s_4 - s_5} = \left(\dot{m}_{s1} + \dot{m}_{s3}\right) \frac{x_{4'} - x_{5'}}{s_4 - s_5}, \text{ kg/(s·m)} \tag{9}$$

where:

$\dot{m}_{s(4-5)}$ — mass stream of dry air in the shaft section 4-5, kg/s. The value has been calculated from the following dependence:

$$\dot{m}_{s(4-5)} = \frac{\dot{m}_{(1-2)}}{1+x_1} + \frac{\dot{m}_3}{1+x_3} = \frac{\dot{m}_1}{1+x_1} + \frac{\dot{m}_3}{1+x_3}, \text{ kg/s} \tag{10}$$

where:

$\dot{m}_1$, $\dot{m}_3$ — mass stream of humid air in the shaft section 1-2, and in cross section 3 of a higher situated shaft bottom, kg/s,

x_1 — specific humidity of air stream at the beginning of the shaft section 1-2, kg/kg,

x_3 — specific humidity of air stream at a higher situated shaft bottom of the given shaft, kg/kg,

$x_{4'}$ — specific humidity of saturated air stream at pt. 4 of the shaft, kg/kg,

$x_{5'}$ — specific humidity of saturated air stream at pt. 5 of the shaft, kg/kg,

s_4 — coordinate corresponding to the position of pt. 4 in the shaft,

s_5 — distance coordinate corresponding to the position of pt. 5 in the shaft.

A unit mass flux of the distributed water source present in section 4-5, has been calculated as:

$$\dot{m}_{W_j(4-5)} = \dot{m}_{s(4-5)} \frac{x_{4'} - x_{5'}}{s_4 - s_5} = \left(\frac{\dot{m}_1}{1+x_1} + \frac{\dot{m}_3}{1+x_3} \right) \frac{x_{4'} - x_{5'}}{s_4 - s_5}, \text{ kg/(s·m)} \tag{11}$$

$$\dot{m}_{W_j(4-5)} = (204,01 + 185,18) \frac{0,0200 - 0,01810}{400} = 0,00185 \text{ kg/(s·m)}$$

At the intersection of the shaft with the ventilation pipe, there is mixing of two air streams: two-phase one of the parameters described at pt. 5 flowing through the shaft with humid air of the parameters demonstrated at pt. 6. Point 6 shows a thermodynamic state of the external air for the pressure corresponding to the pressure value depicted at point 5. The process of mixing such air streams has been presented on the Mollier diagram for the summer and winter periods with the assumption that external air losses in both cases account for 10% of the total volumetric flow rate of the air discharged from the mine. The point illustrating the parameters of the obtained air stream mixture has been marked as number 8 for the summer and number 10 for the winter period. These points correspond to the points 8' and 10' respectively, depicting the thermodynamic state of humid saturated air. Their location with reference to the corresponding position of the points 8 and 10 on the Mollier diagram proves that the resultant stream produced due to the air mixing process is two-phased one. The mass output of the localised water source in the shaft cross section of the s_5 coordinate for the summer period, can be calculated as follows:

$$\dot{m}_{W(5-8)} = 1,1(\dot{m}_{s1} + \dot{m}_{s3})(x_8 - x_{8'}) - (\dot{m}_{s1} + \dot{m}_{s3})(x_5 - x_{5'}), \text{ kg/s} \tag{12}$$

For the winter period the mass output of this water source can be calculated from the formula:

$$\dot{m}_{W(5-10)} = 1,1(\dot{m}_{s1} + \dot{m}_{s3})(x_{10} - x_{10'}) - (\dot{m}_{s1} + \dot{m}_{s3})(x_5 - x_{5'}), \text{ kg/s} \tag{13}$$

where:

x_8, x_{10} — moisture content in air stream after mixing for the summer and winter period, kg/kg,

$x_{8'}, x_{10'}$ — specific humidity of saturated air after mixing for the summer and winter period, kg/kg.

The value of the coefficient 1,1 in the formulas (12) and (13) stems from the assumption that the external losses of the dry air account for 10% of the total dry air stream flowing through the ventilation shaft. The necessary condition for the occurrence of the mass water source resulting from mixing two air streams at the inlet of the ventilation pipe, is to satisfy the following inequalities:

$$\frac{x_5 - x_{5'}}{x_8 - x_{8'}} < 1{,}1\,, \qquad \text{for the summer period,} \tag{14}$$

$$\frac{x_5 - x_{5'}}{x_{10} - x_{10'}} < 1{,}1\,, \qquad \text{for the winter period,} \tag{15}$$

The left sides of the inequalities (14) and (15) calculated from the values read from Fig.5 are 1,138 for the summer and 0,892 for the winter period, respectively. Thus, it appears that the inequality (14) for the summer period is not satisfied. This means that during this time the process of mixing air streams is manifested by a localised water relief in this area of the shaft. In winter the situation is different as a localised mass water source can be observed in the same place. The values of the mass output of the localised water relief in summer, as well as the localised mass water source in winter in sections (5-8) and (5-10), can be calculated respectively as:

$$\dot{m}_{W(5-8)} = 1{,}1\,(204{,}01 + 185{,}18)\,(0{,}0208 - 0{,}0179) + \\ - (204{,}01 + 185{,}18)\,(\,0{,}02140 - 0{,}01810) = -0{,}04281 \text{ kg/s},$$

$$\dot{m}_{W(5-10)} = 1{,}1\,(204{,}01 + 185{,}18)\,(0{,}0195 - 0{,}0158) + \\ - (204{,}01 + 185{,}18)\,(0{,}02140 - 0{,}01810) = 0{,}29968 \text{ kg/s}$$

The phenomenon of mixing the haze air stream containing water mist flowing out from the underground mining excavations (pt. 5) and the humid air stream from the so-called external losses, may lead to the appearance of a localised water relief in the summer, and a localised water source in the winter period.

A ventilation pipe is the last section of the mining air discharge system in which the cooling process takes place. The temperature of the flowing haze air decreases there even further. The process including the change of the air pressure is depicted in Fig. 5 as section 8-11 in summer and 10-12 in winter. Due to the dependencies (16) and (17) observed in the given sections:

$$x_{11'} < x_{8'} \tag{16}$$

$$x_{12'} < x_{10'} \tag{17}$$

a distributed water mass source appears in the ventilation pipe both in the summer and winter periods. Its unit mass output can be calculated using the following formulas:

$$\dot{m}_{W_j(8-11)} = 1{,}1\left(\dot{m}_{s1} + \dot{m}_{s3}\right)\frac{\left(x_{8'} - x_{11'}\right)}{l_{pipe}}, \text{ kg/(s·m), for the summer period} \tag{18}$$

$$\dot{m}_{W_j(8-12)} = 1{,}1\left(\dot{m}_{s1} + \dot{m}_{s3}\right)\frac{\left(x_{10'} - x_{12'}\right)}{l_{pipe}}, \text{ kg/(s·m), for the winter period} \tag{19}$$

After substituting appropriate values from Tab. 1, the dependencies (18) and (19) are:

$$\dot{m}_{W_j(8-11)} = 1{,}1\left(204{,}01 + 185{,}18\right)\frac{\left(0{,}0179 - 0{,}0159\right)}{28} = 0{,}0306 \text{ kg/(s·m), for the summer period}$$

$$\dot{m}_{Wj(8-12)} = 1{,}1\left(204{,}01 + 185{,}18\right)\frac{\left(0{,}0158 - 0{,}0140\right)}{28} = 0{,}0275 \text{ kg/(s·m), for the winter period.}$$

At the section of the ventilation duct connecting the ventilation pipe with the fan (11-K, 12-K), no changes of the air temperature have been observed.

5. Summary and conclusions

The procedure based on the Mollier diagram for variable pressure allows to determine thermodynamic transitions of the air in a ventilation shaft as well as regions where two-phase airflow occurs (of air and water).

Summarising the discussion regarding the water sources induced in the process of water vapour condensation in the return airways, it can be concluded that in the analysed example:

1. Water vapour condensation does not occur over the first 80 metres of section 1-2 of the shaft. However, in the remaining section of the shaft, from the point W to the node 2, both vapour condensation and a water source of the constant mass output, can be observed. The source can be depicted as a continuous distance function.
2. As a result of mixing air streams a water relief occurs in the node 2. The relief can be represented as a local distance function.
3. Water vapour condensation and a water source of constant unit mass output occurs along the entire section 4-5. The source can be depicted as a continuous distance function.
4. In the nodes 8 and 10, the occurrence of a water relief in summer and a water source in winter is the result of mixing external air streams flowing into the mine due to the shaft outset leakage. Both water relief and water source can be represented as local distance functions.
5. In the ventilation pipe, water vapour condensation and a water source can be detected. The water source of the constant unit mass output can be depicted as a continuous distance function. The temperature in the ventilation shaft does not vary and neither water vapour condensation nor a water source occur there. The section's only function is discharge of the two-phase mixture of air and water to the surface.

Acknowledgements

This study was supported by the AGH University of Science and Technology the statutory research No. 11.11.100.920

References

Dziubiński M., Prywer J., 2009. *Mechanika płynów dwufazowych*. WN-T, Warszawa.

Orzechowski Z., Prywer J., Zarzycki R., 2009. *Mechanika płynów w inżynierii i ochronie środowiska*. WN-T, Warszawa.

Ptaszyński B., 2016. *Wykorzystanie wykresu Molliera w analizie przemian powietrza wilgotnego w wyrobiskach górniczych*. Ciepłownictwo, Ogrzewnictwo, Wentylacja 47/9.

Pudlik W., 2011. *Termodynamika*. Wydawnictwo Politechniki Gdańskiej.

Wacławik J., 2010. *Wentylacja kopalń, tom I, II*. Wydawnictwo AGH, Kraków.